Computer-Aided Design and Applications

http://www.cadanda.com

Haptic Rendering of Three-dimensional Heterogeneous Fine Surface Features

Y. H. Chen, L. L. Lian and X. J. He

University of Hong Kong, yhchen@hku.hk, lianlili@hkusua.hku.hk, hexuejian@hkusua.hku.hk

ABSTRACT

Haptic perception of fine surface features is a fundamental modality to identify virtual objects. Roughness and stickiness, which are modeled as surface textures and friction respectively, are the main characteristics in terms of haptics. This research is aimed at the haptic rendering method of fine surface features based on the analysis of the surface profile. Functionally generated surface features are employed for the haptic rendering of surface textures and surface friction. Haptic rendering of anisotropic surface - surface having a dominant feature direction, and haptic rendering of heterogeneous surface - surface with a varied feature density, are investigated. Experimental measurements and prototype system implementations have been done to show the fidelity of the proposed surface feature modeling methods.

Keywords: haptic, fine surface feature, texture, friction.
DOI: 10.3722/cadaps.2008.1-16

1. INTRODUCTION

Different materials present different tactile properties. For instance, it is easier for a hand to slide across an ice surface than a wooden surface. Even for the same material, different finishing processes can result in different surface roughness. Fine surface features, which are not unique to an object though, perception of them is fundamental for identifying objects in the real world, as it should be in a virtual environment. Nowadays, there are many on-going researches about virtual reality or augmented reality. In some of these researches, surface features play a very important role, for instance, in order to have realistic feedback to users, the interaction between objects in virtual environment must consider object surface features because the effect of contact and relative motion between virtual objects are influenced by surface features. In other words, the accurate modeling of virtual objects interaction dictates the modeling of fine surface features.

Current research on haptic rendering of fine surface features focuses on surface friction and surface textures. With the development of haptic rendering techniques and the availability of general-purpose commercial haptic devices, e.g. PHANToM®, researchers are no longer satisfied with only visual perception of a virtual scene or objects. Tactile perception has been actively investigated in recent years [1, 2].

1.1 Haptic Rendering of Friction

To some extent, friction is present in all sliding objects and mechanisms with sliding parts. Including friction in haptic rendering of virtual objects can not only increase the realism of the interaction, but also help the user to distinguish different kinds of materials and surface roughness. Armstrong made an extensive survey on friction models in [3].

There are a number of well-known friction models. The most commonly used friction model is the linear viscous damping model. It models the friction as being proportional to the sliding velocity. Although this model is effective in sliding sticky or oily surfaces, it can not simulate the "stick slip" phenomenon caused by the static friction. Another commonly used model is the Coulomb's model. This model states the friction is proportional to the normal constraint force and opposes the slip velocity when the sliding velocity is non-zero. The zero velocity condition is maintained by setting the static friction as any necessary value within the static friction limit. This method is used in the haptic

rendering of friction in [4, 5]. But it has an obvious drawback - The hard non-linearity at zero velocity makes efficient computer simulation of friction difficult, which may cause small force oscillations around the small zero-velocity area when applied in haptic simulation. This problem can be overcome by using Karnopp's friction model. In Karnopp's model, within the small zero-velocity area, the friction is calculated as the minimum value between the value needed to keep the system at zero velocity and the break-away friction force level. Based on Karnopp's model, Berkelman and Richard achieved stable haptic rendering of friction [6, 7].
Dahl modeled friction as a function of displacement [8]. The model states that the rate of change of friction with respect to time is equal to the rate of change of friction with respect to position multiplied by the relative velocity of the two moving bodies. Because this model is position based and does not have high requirement for the velocity resolution which is difficult for the haptic interface to meet, it is suitable for haptic simulation purpose. Hayward and Armstrong implemented robust haptic rendering of friction based on this model [9]. They improved Dahl's method by adding a virtual spring between a stationary surface and a sliding object. Stretching of the spring determines the transition from static to sliding state and realistic viscoelastic behaviors are also produced.
Friction results from the contact and sliding between micro textures of surfaces in contact, but effect of texture patterns on the friction is seldom considered by previous research. Further more, current haptic rendering methods of friction only apply to isotropic and homogeneous surfaces. In reality, anisotropic and heterogeneous surfaces widely exist. Haptic rendering of friction on such surfaces is what this research focuses on.

1.2 Haptic Rendering of Textures

Current research on haptic rendering of textures, or known as haptic texturing, is in fact the rendering of tiny bumps or other tiny geometrical features at the scale of millimeters. The first convincing and realistic haptic display of textures was implemented by the 'sandpaper' system [10, 11]. In the 'sandpaper' system, haptic textures are simulated using only the lateral forces with a 2 DOF force reflecting joystick. Roughness perception is achieved by generating lateral forces proportional to the local gradient of a simulated bumpy surface.
The first step to haptically display textures is texture generation. Either image-based method or procedural method can be used. In image-based method, a two-dimensional image is mapped onto a three-dimensional surface and the gray scale intensities are directly used to generate a height field that can be used in the haptic rendering. While in the procedural method, the height field is generated by mathematical functions, e.g. Gaussian function or Fourier series. The second step is to display the height field by certain kind of haptic rendering technique. Current methods of haptic texturing can be considered as the following two categories.
(a) Geometry-based method. Some researchers treat surface textures in the same way as rigid objects. Surface textures are represented by geometry models, e.g. polygon meshes. Contact with these meshes results in a responsive force normal to the surface, which gives the user sensations of roughness.
McGee et al. presented a multimodal perception method of virtual roughness in [1]. They generated haptic textures as sinusoidal waves on a rectangle patch, so the profile of the texture was dependent on the amplitude and frequency of the waves. The user felt a bump at the peak of each wave. Otaduy and Lin proposed a perceptually-inspired 6DOF force model for haptic texture rendering [12]. To reduce the computation cost, they used approximate geometric representations for surface textures. The reaction force and torque that produce the texture force is dependent on the gradient of penetration depth of the virtual probe. Psychophysical factors including the probe diameter, the applied force, and the exploratory speed are considered to generate realistic perceptions.
The principle of the geometry-based haptic texturing method is straightforward and it is in conformity with the inherent nature of surface textures. But accurate geometry representation of fine surface features is not a trivial job. Furthermore, representation with high resolution (more detail of surface features) will increase the burden of collision detection and haptic rendering, both of which run at a very high rate in the haptic simulation.
(b) Force perturbation method. In this method, the textured surface is geometrically represented by a smooth surface, and texture patterns are directly mapped to the smooth surface. To get roughness perceptions, contact forces are varied according to the texture mapping. The 'sandpaper' system is an example that makes use of this method.
Another system based on force perturbation was implemented by Siira and Pai [13, 14]. They developed a stochastic approach for haptic rendering of textures. According to their definition, haptic textures are all the effects which are not explicitly accounted for by rigid body contact and friction forces. They observed that many surface preparation methods resulted in roughness profiles which were approximately Gaussian function, therefore Gaussian function was used to model the texture force map. The model with only lateral forces that is similar to that in 'Sandpaper' is used for haptic rendering. To haptically display more fractal surfaces, Costa and Cutkosky proposed a dynamic model that represented the normal and tangential forces [15]. Both a damper and a spring were added between each pair of crest

and nadir of the texture map, thus the feeling of waviness was created and bouncing or skipping over the valleys, which were commonplace for fractal surfaces, was avoided.
The force perturbation method is more computationally efficient compared with its counterpart. But it requires the decomposition of the contact force and the realism of the texture forces is dependent on results of appropriate psychophysical experiments. Due to the difficulties in modeling the realistic force feedback in haptic texturing, some researchers have tried to record the surface textures of real objects and play them back as haptic textures [16, 17]. These efforts are currently reported on planar surfaces only. It is also difficult to extend this method to surfaces with multiple texture patterns.
In this paper, the lateral-force method is improved so that the texture forces are consistent with the geometrical nature of the textured surface. It is further extended to model texture forces on 3D surfaces. The paper is organized as follows: Section 2 is an analysis of the surface profile and the contact forces. The analysis lays the theoretical foundation for the proposed haptic rendering method. Section 3 focuses on systematic generation of fine surface features. Section 4 and section 5 describe the haptic rendering algorithms of friction and textures based on the generated surface features, respectively. Section 6 makes a conclusion briefly.

2. MODELING OF CONTACT FORCES

2.1 Analysis of the Surface Profile

On a micro scale, surfaces of almost all objects are not smooth. They often have little bumps arising from a relatively homogeneous substrate. Depending on the size of or space between the bumps, fine surface features can be classified into micro features and macro features [18]. In a micro feature of machined surfaces, the bumps are spaced at intervals of the order of micron (10^{-6}m). It often results from the microstructure of the material and action of the cutting tool. R_a (Roughness Average) and R_q (Root Mean Square Roughness) are the most important parameters to evaluate the amplitude of the micro features. In a macro feature, the size is of the order of millimeter (10^{-3}m). Machine or work deflections, vibrations, and larger material structures (e.g. bumps on wood or rock) result in macro features. When the bumps get sparser, they can be modeled as geometrical primitives. Micro features, macro features, and basic shapes compose the real object surface altogether (Fig.1).

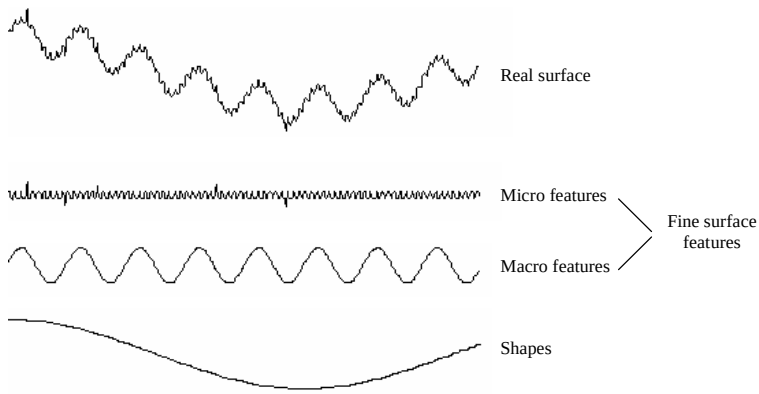

Fig. 1: Surface profiles.

2.2 Modeling of Contact Forces

In haptic simulation, according to the scale of the surface features, contact forces between the virtual probe and the virtual objects are modeled as friction, texture force, and rigid body constraint as in Tab.1. Perception of basic surface shapes is modeled as rigid body constraint. Haptic rendering of normal constraint generates an illusion of surface hardness of a smooth and frictionless object. Micro features are haptically displayed by friction using one of the models as introduced in section 1.1. In most cases, both the geometry representation of an individual bump and the distribution of the bumps are neglected, and the frictional surface is regarded as homogeneous. Adding friction to the normal constraint creates a smooth and frictional surface. Macro features are represented by textures, or sometimes referred to as roughness. Haptic rendering of these features is often called haptic texturing. Texture forces are rendered

using either the geometry-based method or the force perturbation method as reviewed in section 1.2. Adding texture forces into the contact force model achieves the perception of a rough surface.
Based on the above analysis, contact forces between the virtual probe and the virtual model can be described by Eqn.(1), and the comparison of different categories of surface features and the corresponding force models are generalized in Tab. 1.

$$F_{contact} = F_{constraints} + F_{friction} + F_{texture} \quad (1)$$

where $\boldsymbol{F}_{\text{contact}}$ is the contact force, $\boldsymbol{F}_{\text{constraints}}$ is the component of constraint force, $\boldsymbol{F}_{\text{friction}}$ is the component of friction force, and $\boldsymbol{F}_{\text{texture}}$ is the component of texture force.

	Micro features	*Macro features*	*Shapes*
Caused by	***Microstructure of the material, the action of the cutting tool, etc.***	***Machine or work deflections, vibrations, larger material structures, etc.***	***Basic shapes***
Wavelength (m)	***10-6***	***10-3***	***>10-3***
Geometry representation	***Height field***	***Height field***	***Primitives***
Force modeling	***Friction***	***Texture force***	***Rigid body constraint***

Tab. 1: Surface features and their force modeling methods.

3. GENERATION OF FINE SURFACE FEATURES

As illustrated in Tab. 1, in this research, height field will be developed to represent the distribution of little bumps. Basically speaking, generation of three-dimensional fine surface features follows two steps. Firstly, two-dimensional models are created using a procedural method that employs mathematical functions to create synthetic features. Two basic types of features–gratings and grids as illustrated in Fig. 2 are generated based on the cosine function. Secondly, the two-dimensional models are 'mapped' to the targeted three-dimensional surface using the shrinkwrap method that is similar to texture mapping in computer graphics. Through the mapping, procedurally generated uniform features can be transformed into heterogeneous ones with varied wavelengths and distribution densities.

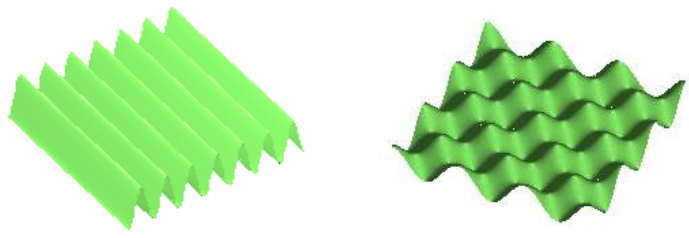

(a) Gratings (b) Grids

Fig. 2: Two fine surface features.

3.1 Two-dimensional Fine Surface Features

To obtain a rough surface, at an arbitrary position (u, v) on the surface, two values are defined to describe the geometry characteristic of the feature–height h and the gradient of height ∇h. The height field from cosine function is used to represent the roughness of the surface. The reason for selecting the cosine function is that it is the basic component of Fourier synthesis which can be used in both micro modeling of intricate details and macro modeling of larger scale structures [18]. The gradient of height is defined by Eqn.(2),

$$\nabla h = grad(h) = \left(\frac{\partial h}{\partial u}, \frac{\partial h}{\partial v}\right) \quad (2)$$

3.1.1 Gratings

Gratings present alternating linear raised bars and valleys, it is one of the most commonly met features in real life. Machining processes, such as planning, milling and turning, can produce surfaces with regular gratings. Height h and the height gradient ∇h of unidirectional gratings and circular gratings are formulated in Eqn.(3) and Eqn.(4), respectively,

$$h(u,v) = c \cdot \cos \omega_0 u, \quad \nabla h = (-c\omega_0 \cdot \sin \omega_0 u, 0), \; u,v \in [0,1] \tag{3}$$

$$h(u,v) = c \cdot \cos(\omega_0 \sqrt{u^2+v^2})$$

$$\nabla h = (-\frac{c\omega_0 \cdot \sin(\omega_0 \sqrt{u^2+v^2}) \cdot u}{\sqrt{u^2+v^2}}, -\frac{c\omega_0 \cdot \sin(\omega_0 \sqrt{u^2+v^2}) \cdot v}{\sqrt{u^2+v^2}}) \tag{4}$$

$$u,v \in [0,1]$$

where c is the amplitude, w_0 is the frequency.

3.1.2 Grids

Grids are represented by raised bumps and valleys in a checker-board pattern. Its height field and height gradient field are defined by Eqn.(5),

$$h(u,v) = c \cos \omega_u u \cdot \cos \omega_v v$$

$$\nabla h = (-c \sin \omega_u u \cdot \cos \omega_v v, -c \sin \omega_v v \cdot \cos \omega_u u), \quad u,v \in [0,1] \tag{5}$$

where c is the amplitude, w_u and w_v are the frequencies along direction u and direction v, respectively.

3.2 Three-dimensional Feature Mapping

The mapping of two-dimensional fine surface features to three-dimensional surfaces is very similar to the process of traditional texture mapping in computer graphics. The shared problem is to correlate the attribute at an arbitrary position (u, v) on the two-dimensional surface with the attribute at position (x, y, z) on the three-dimensional object. The difference lies in that, in texture mapping, the attributes are usually RGB values which are not affected by the mapping process; whereas in the mapping of surface features, the attributes include the height and the height gradient, the later of which is partially dependent on the geometry of the targeted surface.

Therefore, an improved Shrinkwrap mapping method is adopted. Details about the Shrinkwrap mapping method can be found in [19]. In the improved Shrinkwrap method, feature mapping is implemented in two stages. The first stage is a mapping from the two-dimensional feature space (represented by $T(u, v)$) to a cylinder surface (represented by $T'(x_i, y_i, z_i)$, which is called the intermediate surface. Any point on the intermediate surface with radius r_i and height l can be represented by $(x_i, y_i, z_i) = (r_i \cos\theta_i, r_i \sin\theta_i, z)$. Therefore, (u, v) which represents an arbitrary point on the two-dimensional feature can be associated with a point on the cylinder by $(u,v) = (\frac{\theta_i}{2\pi}, z)$.

The second stage maps the three-dimensional features on the cylinder to the object surface (represented by $O(x, y, z)$). This stage can be implemented by a ray tracing method. As illustrated in Fig.3, a ray whose orientation is given by the intermediate surface normal at (x_i, y_i, z_i) is drawn from (x, y, z) on the targeted surface to (x_i, y_i, z_i) on the intermediate surface. Therefore, (θ, r, z), which is the corresponding point of (x, y, z) in the cylindrical space can be associated with a point on the intermediate surface by $(\theta, r, z) = (\theta_i, r_i, z_i)$.

Once the relationship is set up, the height h and the gradient of height ∇h at (θ, r, z) can be formulated as,

$$h_O(\theta, r, z) = h_{T'}(\theta, r, z) = h_T(\frac{\theta}{\theta_2 - \theta_1}, \frac{z}{z_2 - z_1}), \theta \in [\theta_1, \theta_2], z \in [z_1, z_2] \tag{6}$$

$$\nabla h_O(\theta, r, z) = (\frac{\partial h_O}{\partial \theta}, \frac{\partial h_O}{\partial r}, \frac{\partial h_O}{\partial z}) \tag{7}$$

In most cases, the virtual environment is created in the Cartesian space, so the height gradient as formulated in Eqn.(8) is desired.

$$\nabla h_O(x,y,z) = (\frac{\partial h_O}{\partial x}, \frac{\partial h_O}{\partial y}, \frac{\partial h_O}{\partial z}) \tag{8}$$

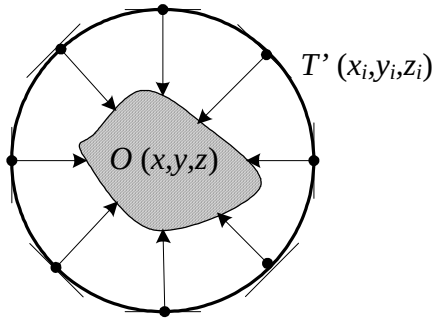

Fig. 3: O-mapping based on intermediate surface normal.

To transform Eqn.(7) from the cylindrical space into the Cartesian space, the chain rule of differentiation is employed. According to the chain rule,

$$\frac{\partial h_O}{\partial x} = \frac{\partial h_O}{\partial \theta} \cdot \frac{\partial \theta}{\partial x} + \frac{\partial h_O}{\partial r} \cdot \frac{\partial r}{\partial x} \tag{9}$$

Similar results can be obtained for $\frac{\partial h_0}{\partial y}$ and $\frac{\partial h_0}{\partial z}$. Replacing Eqn.(9) into Eqn.(8), the height gradient in the Cartesian space can be obtained.

3.1.3 An example

Let the unidirectional gratings be represented by $h(u,v) = 0.01\cos 20u, \quad u,v \in [0,1]$. Map the gratings to an object surface *O*(*x, y, z*) (Fig. 4) as formulated by

$$x = r \cdot \cos\theta, y = r \cdot \sin\theta, z = r^3 + 3\theta, \theta \in [0,\pi], r \in [1,3].$$

According to Eqn.(6) and Eqn.(8), the height field and height gradient field can be calculated by the followings,

$$h_O(\theta,r,z) = 0.01\cos(\frac{20\theta}{\pi})$$

$$\nabla h_0(x,y,z) = (\frac{\partial h_0}{\partial \theta} \cdot \frac{\partial \theta}{\partial x}, \frac{\partial h_0}{\partial \theta} \cdot \frac{\partial \theta}{\partial y}, \frac{\partial h_0}{\partial \theta} \cdot \frac{\partial \theta}{\partial z}) = \frac{\sin(\frac{20}{\pi}\arctan\frac{y}{x})}{5\pi(x^2+y^2)} \cdot (y, -x, -\frac{\sqrt{x^2+y^2}}{3})$$

The results are illustrated in 5 and 6. In Fig. 5, the color represents the height of fine surface features on the surface. In Fig. 6, the gradient of height is displayed by the red arrow. From these two figures, it can be seen that the three-dimensional feature mapping can result in heterogeneous fine surface features with varied spatial density and irregular feature layout. The method of displaying such features haptically will be introduced in detail in section 4 and section 5.

4. HAPTIC TEXTURING

As mentioned previously, fine surface features in the millimeter scale are referred to as surface textures, or roughness by some researchers. Haptic rendering of such features is known as haptic texturing. In this research, haptic rendering of textures is implemented based on the lateral-force method used in the 'sandpaper' [10]. And the method is improved in three aspects: Firstly, rather than being constrained to two-dimensional surfaces, we extend the method to three-dimensional ones by using the 6DOF haptic device PHANToM®. Furthermore, based on our feature mapping algorithm, the developed method makes it possible to haptically render heterogeneous fine surface features with varied spatial density and irregular feature layout. And finally, the effect of normal force is incorporated in the algorithm to make it consistent with the geometrical nature of the textured surface.

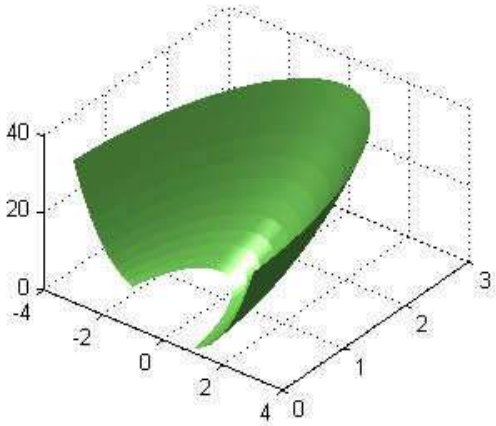

Fig. 4: Sample surface.

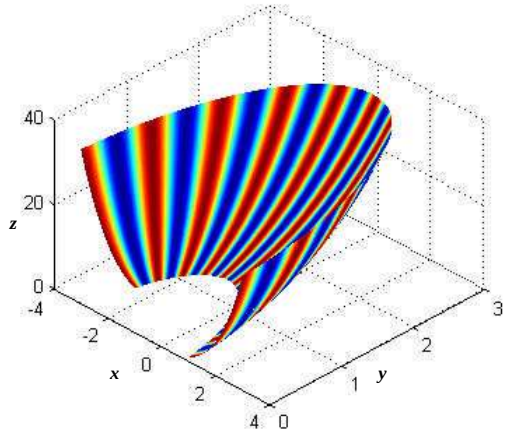

Fig. 5: Height fields of the sample surface.

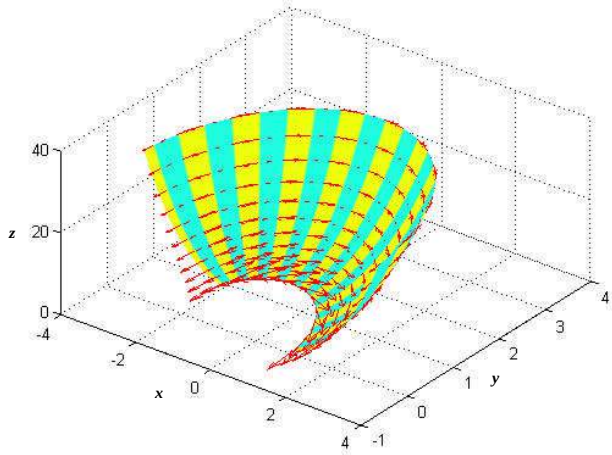

Fig. 6: Height gradient fields of the sample surface.

4.1 Lateral-force Algorithm

The lateral-force method was proposed by Minsky and Lederman [11]. The principle of this method lies in the observation that sideway spring force can feel like downward force. In other words, a spring potential field feels like a deep valley with a center at the rest position of the spring. Therefore, in a human haptic system, having the hand pulled down by gravity into a valley can be analogical to having the hand pulled toward a point of the rest position.

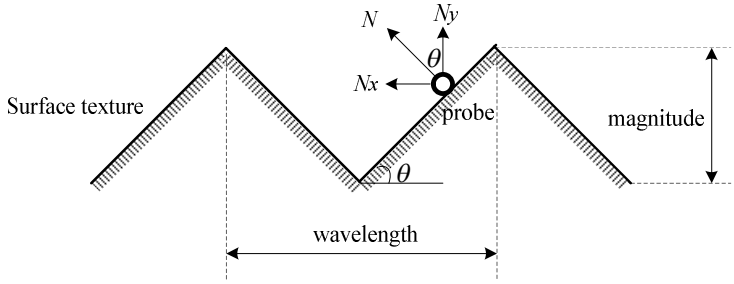

Fig. 7: Lateral-force algorithm.

Historically, the lateral-force algorithm is arrived as the outcome of the perceptual observation. Here it is interpreted in the physical model as shown in Fig.7. In Fig.7, textures composed of triangular ridges with the slope angle θ are generated. The virtual probe is manipulated to slide across the textured surface. If there is no friction between the surface and the probe, ideally, it is expected that force N which is normal to the surface is presented to achieve the sensation of textures. This is the theoretical basis of geometry-based haptic rendering method of textures. When the lateral-force algorithm is utilized, only the lateral force N_x is displayed. It can be calculated based on the constraint force N_y.

$$N_x = N_y \tan\theta \tag{10}$$

where θ is the slope angle of the ridge, N_y is the constraint force of the rigid shape. In our system, by rendering the lateral force N_x and the constraint force N_y separately and concurrently, the same effect as direct rendering of the resultant force N can be achieved.

Let the height field of the texture be represented by $h=h(x)$, the lateral force can be calculated from Eqn.(11),

$$N_x = -\frac{\partial h}{\partial x} \cdot N_y \tag{11}$$

When extending Eqn.(11) to a three-dimensional space, it is formulated as Eqn.(12),

$$N_x = -\nabla h \cdot N_y \tag{12}$$

where h is the height field, is the gradient ∇h of the height field which can be formulated as introduced in section 2.

4.2 Implementations

A prototype system is implemented using a PC controlled desktop PHANToM® (Fig.8). The computer has dual CPUs that each runs at 2.0G Hz. The RAM space is 1G. GHOST® API provided by SensAble® Technologies as a user interface is employed to develop the virtual environment.

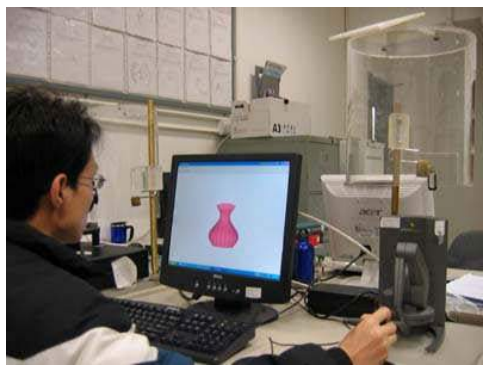

Fig. 8: The prototype system.

Three types of textures are generated. They are two-dimensional unidirectional gratings, two-dimensional grids, and the three-dimensional heterogeneous gratings. For each type of texture, the amplitude and the wavelength can be selected by the user. The range of the wavelength varies from 0.5 *mm* to 5 *mm*. Determination of the range is based on two aspects. Firstly, from the view of psychophysics, geometrical features with the size around 5 *mm* or larger are considered as small shape features rather than textures. And secondly, it is restricted by the position resolution of the haptic device because a too small wavelength can not ensure there are enough different levels of force that can be displayed. Taking the triangular texture in Fig.10 as an example, if the wavelength is 0.5 *mm*, twenty-five different levels of force can be displayed when using PHANToM® desktop whose position resolution is 0.02 *mm*. When the wavelength is decreased to 0.1 *mm*, only five different levels of force can be displayed, which makes the texture feel imprecise.

In order to test the system performance, firstly, the probe is pulled to slide across a smooth surface. The contact force or the constraint force against sliding distance is illustrated in Fig.9. It can be seen that the constraint force varies slightly without visible patterns because of the minor shaking of the user's hand. Then the probe is pulled to slide

across two rectangular surfaces with unidirectional gratings: one surface with a magnitude and wavelength of 0.5 *mm* and 5 *mm* respectively; and the other with 0.5 *mm* and 2.5 *mm* respectively. Fig.10 illustrates the relationship between the lateral force and sliding distance for the two surfaces. It can be seen from the figure that even though the two textures have the same magnitude, the one with smaller wavelength exhibits larger force variation.

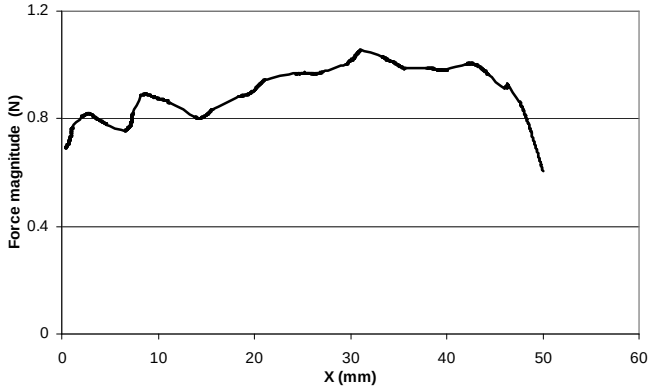

Fig. 9: Constraint force of a smooth surface.

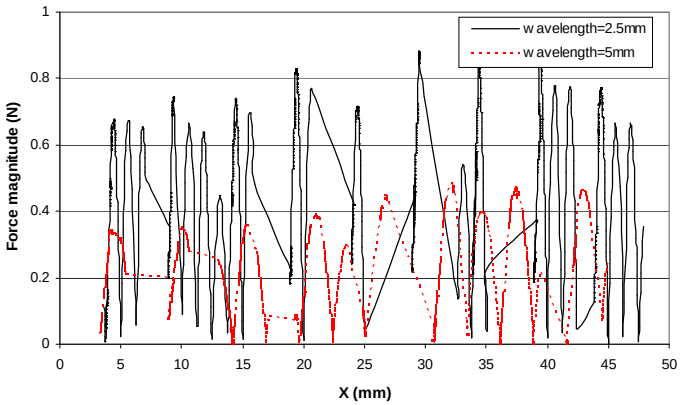

Fig. 10: Lateral force change against sliding distance.

Fig. 11(a) shows a vase-shaped object to which the unidirectional gratings are mapped. After feature mapping, the wavelength of the textures varies from 1.5 *mm* to 4.5 *mm*. The densest gratings occur at the 'neck' and the sparsest ones occur near the bottom as pointed out in the figure. The uneven distribution of the gratings leads to heterogeneous roughness throughout the surface. Three users were invited to experience the haptic textures using the developed system. They all expressed that the 'neck' of the object felt smoothest and the 'abdomen' felt roughest even though the magnitudes (depth) of the textures are the same. This result corresponds to the psychophysical observations that the perceived roughness increases with the increase of the inter-element space within a certain range [20]. In Fig.1(b), the relationship between lateral force and sliding distance is plotted. It can be seen that even though the texture depth magnitude is the same, yet the perceived force variation at the neck is much larger. The larger force variation does not necessary gives the user the feeling that the touched portion is rougher. This may be explained as when the wave length is small, the user can longer feel the force change when sliding on the surface. It will be interesting to do some psychological experiments to find out the relationship between psychological roughness and the actual numerical roughness of a surface.

5. HATPIC RENDERING OF FRICTION

When the wavelength of the surface features decreases to the scale of micron (10^{-6} *m*), roughness of the surface is often evaluated by R_a (Roughness Average) and R_q (Root Mean Square Roughness). Exploration of micro surface features at this scale causes the sensation of friction instead of surface detail. If the influence of factors such as the

lubricant and the temperature is ignored, surface friction is mainly associated with surface roughness [21]. Therefore, in this research, haptic rendering of friction is based on surface roughness represented by the fine surface features generated in section 3. And the haptic rendering algorithm in this research is expected to achieve two aims: Firstly, the friction is stable and can simulate the stick-slide effect; and secondly, it applies to not only isotropic and homogeneous surfaces, but anisotropic and heterogeneous surfaces too.

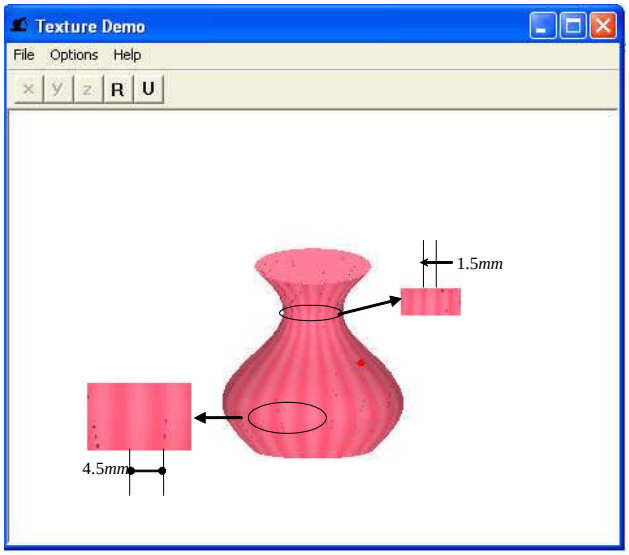

(a) Gratings mapped to a vase surface.

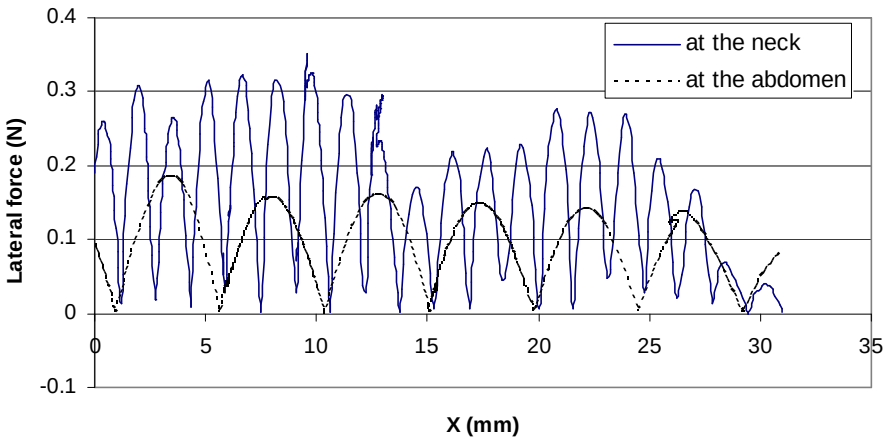

(b) Lateral force change against sliding distance.

Fig. 11: Texture perception of a vase.

5.1 Friction Model

The friction model is based on the Karnopp's method and is illustrated in Fig.12. At time t, when it is detected that the virtual probe collides with the virtual object, the relative velocity between them at the contact point is calculated. If it is less than Δv, the system state is considered 'stick', and the static friction is presented to the operator. Theoretically, the static friction is equal to the applied force to keep the probe staying at the original position. However, it is difficult to be

implemented because the haptic device can only map positions to forces, not vice versa. Therefore, the static friction is calculated according to the change of the positions as formulated in Eqn.(13),

$$\vec{f}_{static} = \min(-k_s \cdot (\vec{P} - \vec{P}'), F_s) \tag{13}$$

where k_s is the static friction coefficient, $\vec{P}$ is the position of the probe at time t, $\vec{P}'$ is the position where the stick occurs, F_s is the maximum static friction.

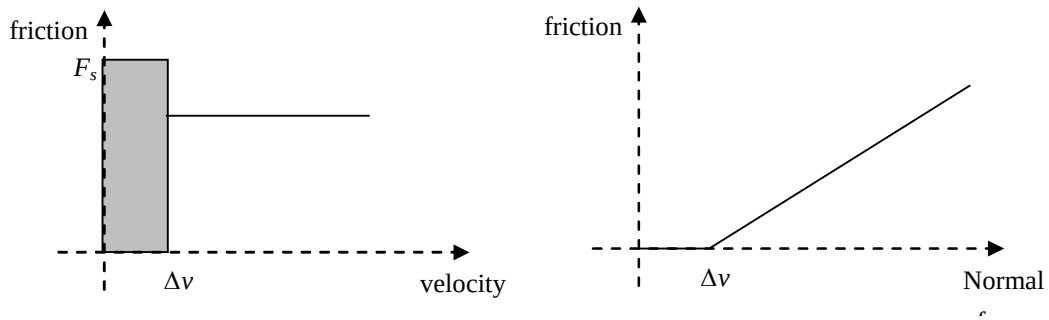

Fig. 12: The friction model.

As the applied force increases to be greater than the threshold of the static friction, the probe will slide across the surface, and the dynamic friction is presented. The dynamic friction displays the effect of Coulomb friction as formulated in Eqn.(14),

$$\vec{f}_{dynamic} = -k_d \cdot |N| \cdot \frac{\vec{v}}{|v|} \tag{14}$$

where k_d is the dynamic friction coefficient, $\vec{v}$ is the velocity of the probe, N is the normal constraint force.

5.2 Haptic Rendering of Heterogeneous Frictional Surface

For most objects, the friction coefficients are not the same throughout the surface. A machined surface often has the minimum roughness along the direction of the cutting path and the maximum roughness perpendicular to the direction of the cutting path. Fig.13 shows an example. The steel surface as shown in Fig.13(a) was obtained by plunge milling and it presented clear unidirectional lay. Roughness of the surface was measured by Mitutoyo-SV3000 as shown in Fig.13(b). Original evaluation data of Ra are illustrated in Fig.13(c) and (d). Fig.13(c) shows the data along the horizontal direction, and Fig.13(d) shows the data along the vertical direction. Based on these measurement data, calculation of R_a gave the results of 3.81μm along the vertical direction and 0.33 μm along the horizontal direction. Obviously, the significantly varied roughness will lead to different friction across the surface.

To haptically display the friction variations of such surfaces, the fine surface features generated in section 3 are employed. Two-dimensional gratings are employed to represent anisotropic surface and their three-dimensional mapping can represent a heterogeneous surface feature with varied dominant direction of gratings.

Then the friction coefficient represented by C (k_d or k_s) is interpolated linearly along different directions (Fig.14),

$$C = C_{\max} - \frac{C_{\max} - C_{\min}}{\pi / 2} \cdot \theta \tag{15}$$

where C_{max} is the maximum of C, which occurs along the direction of height gradient ∇h (refer to Section 3.1), C_{min} is the minimum of C, which occurs perpendicular to the direction of ∇h , and θ is the acute angle between the probe velocity and ∇h. For two-dimensional gratings, it can be calculated by Eqn.(3) and Eqn.(4); for three-dimensional gratings, it can be calculated by Eqn.(8). Using the interpolated friction coefficient to replace the constant coefficient in Eqn.(13) and Eqn.(14), anisotropical and heterogeneous frictional surfaces can be displayed haptically.

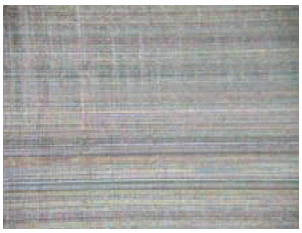

(a) Anisotropic surface

(b) Friction measurement

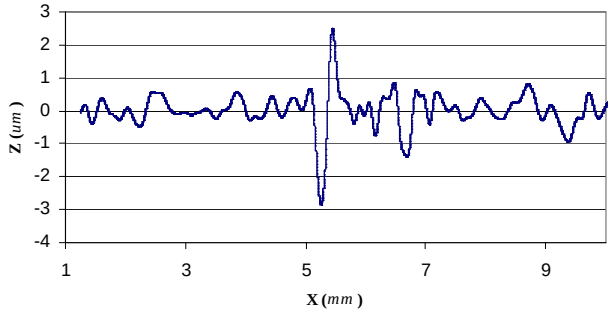

(c) Horizontal evaluation data

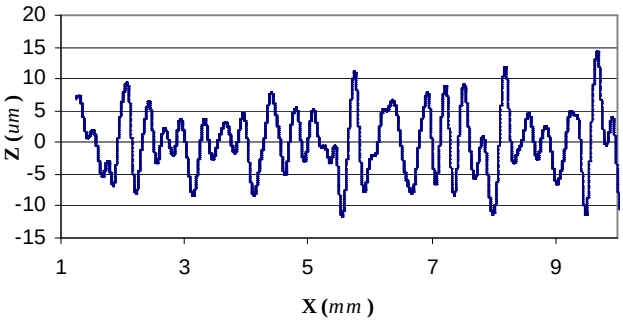

(d) Vertical evaluation data

Fig. 13: An anisotropic surface.

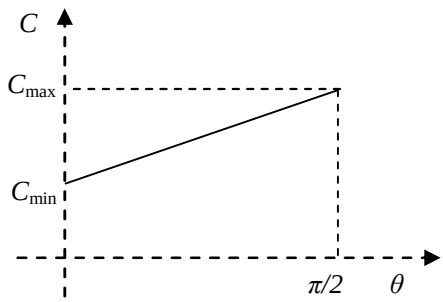

Fig. 14: Linear interpolation of friction coefficients.

5.3 Implementations

A prototype system based on the same hardware as described in section 4.2 is developed to perceive fine surface features based on the above friction model. The first test is on two-dimensional homogeneous and isotropic surface. Two simulations using the parameters as illustrated in Tab.2 are done. The results are shown in Fig.15. The figure illustrates the stick-slide phenomenon clearly: When the velocity of the probe is less than Δv, static friction is displayed. This stage will last until the applied force exceeds the static friction threshold and the system state transfers to 'slide'. At the transition point, the displayed friction drops sharply which provides the operator a strong sense of transition from

the stick state to the slide state. Even though the parameters in the two simulations are different, the results in Fig.15 show similar patterns (The patterns can not repeat themselves as the user can not repeat the applied force and velocity).

	k_s (N/mm)	k_d	Δv (mm/s)	Static friction threshold (N)
Simulation 1	0.25	0.4	5.0	0.4
Simulation 2	0.30	0.6	5.0	0.6

Tab. 2: Simulation parameters.

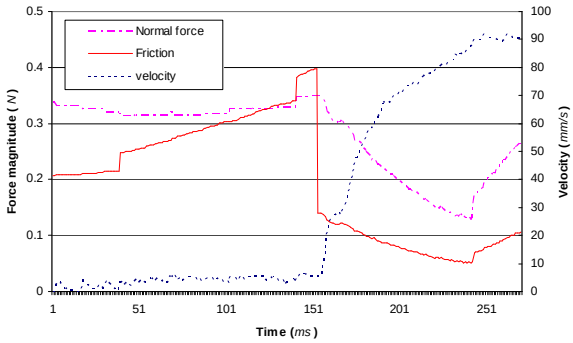

(a) Simulation 1

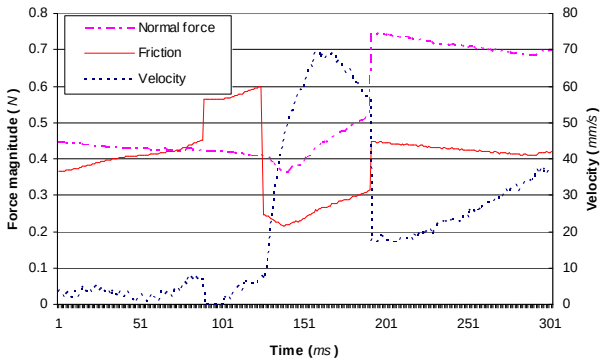

(b) Simulation 2

Fig. 15: Haptic rendering of friction of homogeneous surface.

Direction	k_s (N/mm)	k_d	Δv (mm/s)	Static friction threshold (N)
Horizontal	0.25	0	5.0	0.4
Vertical	0.25	0.4	5.0	0.4

Tab. 3: Simulation parameters for anisotropic surface features.

Fig.16 shows a machined metal block with anisotropic surface features. In this simulation, the frictional surface is the roughest along the vertical direction and the smoothest along the horizontal direction. For better comparison, an extreme condition is adopted by setting the horizontal direction completely smooth. To exclude the effect of the normal force variation on the friction, it is set to 0.6 *N* throughout the simulation. Other parameters used in the simulation are illustrated in Tab.3. The probe slides across the surface along different directions as shown in Fig.16 (a) and (b). When the trajectory is nearly horizontal (Fig.16 (a)), the dynamic friction is almost equal to zero (Fig.17 (a)), and the user feels a smooth surface. When the trajectory turns more towards vertical (Fig.16 (b)), the dynamic friction

gets larger (Fig.17 (b)), and a rougher surface is perceived. It can be seen that the proposed model complies with actual perception.

(a) (b)

Fig. 16: Trajectory of the probe.

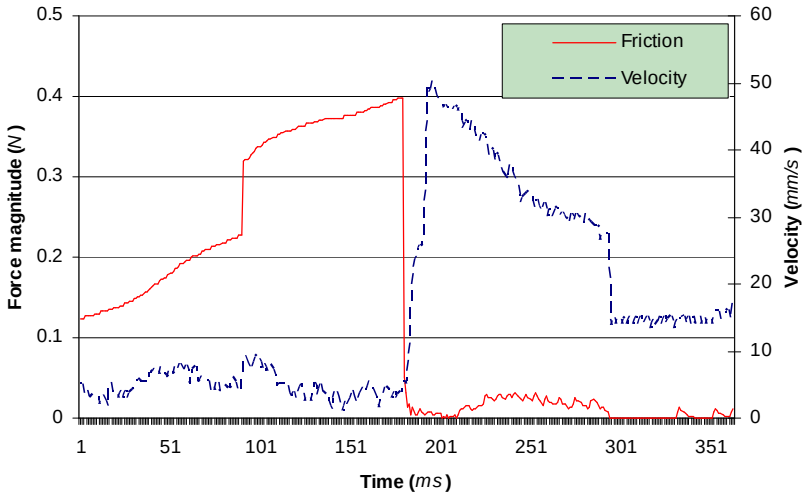

(a) Simulation for Fig.16 (a).

6. CONCLUSIONS

In this research, haptic rendering algorithms for fine surface features are developed. Different from traditional methods which regard surface textures and surface friction as completely different features, our haptic rendering method is based on the uniform representation of fine surface features. The height field and height gradient field for different types of features are defined systematically.

The uniform representation of fine surface features has two advantages: Firstly, it clarifies the inherent geometry of surface profiles. A surface profile consists of features of different size-micro feature, macro feature, and shape. Although friction and texture force exhibit totally different behaviors, they are both modeled as the tactile perception of fine surface features, and the difference comes only from the size of the features. Secondly, the uniform representation makes it possible to haptically display anisotropic and heterogeneous friction. Previous research has always neglected the heterogeneous property of friction, and surface friction was treated as isotropic and homogeneous. Based on the height gradient field of surface features, anisotropic friction and heterogeneous friction can be haptically perceived. The haptic perceptions are tested based on two prototype systems implemented during the course of research.

Another contribution of this research is that the lateral force algorithm for haptic texturing has been extended to 3D heterogeneous surface features by taking into account of the normal force feature mapping. Via feature mapping, heterogeneously textured surface features (irregular distribution and varied spatial density of gratings) can be obtained.

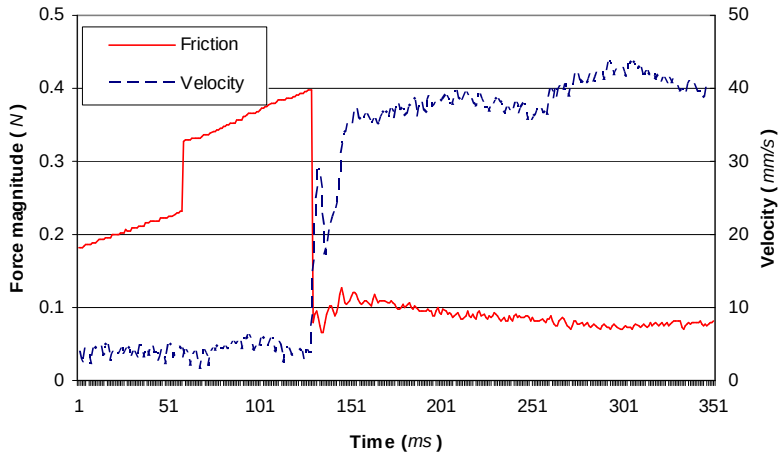

(b) Simulation for Fig.16 (b).

Fig. 17: Haptic rendering of friction of anisotropic surface.

7. ACKNOWLEDGEMENTS

This research is supported by a grant from Hong Kong Research Grants Council under the code HKU 7116/05E.

8. REFERENCES

[1] McGee, M. R.; Gray, P. D.; et al.: Mixed Feelings: Multimodal Perception of Virtual Roughness, Proceedings of Eurohaptics Edinburgh, UK, 2002.

[2] Omar, A.; Dominguez R.; et al.: Texture, Roughness, and Shape Haptic Perception of Deformable Virtual Objects with Constrained Lagrangian Formulation, Intl. Conference on Intelligent Robots and Systems, Las Vegas, Nevada, 2003.

[3] Armstrong-H'elouvry; Dupont B., P.; et al.: A survey of models, analysis tools and compensation methods for the control of machines with friction, Automatica, 30(7), 1994, 1083-1138.

[4] Kry, P. G.; Pai, D. K.: Continuous Contact Simulation for Smooth Surfaces, ACM Transactions on graphics, 22(1), 2003, 106-129.

[5] Pai, D. K. etal: Scanning Physical Interaction Behavior of 3D Objects, Computer Graphics (ACM SIGGRAPH 2001 Conference Proceedings, 2001.

[6] Berkelman, P.: Tool-Based Haptic Interaction with Dynamic Physical Simulations using Lorentz Magnetic Levitation, Pittsburgh, PA, Carnegie Mellon University, Ph.D theis, 1999.

[7] Richard, C.: On the identification and haptic display of friction. Mechanical engineering, Stanford University, Ph. D thesis, 2000.

[8] Dahl, P. R.: Solid friction damping of mechanical vibrations, Am. Inst. Aeronaut. Astronaut. J., 14(12), 1976, 1675–1682.

[9] Hayward, V.; Armstrong, B.: A new computational model of friction applied to haptic rendering, Experimental Robotics VI. Corke and J. Trevelyan, New York, Springer, 2000, 404-412.

[10] Minsky, M.; Lederman, S. J.: Simulated Haptic Textures: Roughness, ASME Journal of Dynamic Systems and Control Division, 58, 1996, 421-426.

[11] Minsky, M.; Ouh-young, M., et al.: Feeling and Seeing: Issues in Force Display. Symposium on Interactive 3D Graphics, Proceedings of the 1990 symposium on Interactive 3D graphics, 1990.

[12] Otaduy, M. A.; Lin, M. C.: A Perceptually-Inspired Force Model for Haptic Texture Rendering, Proc. of the Symposium on Applied Perception in Graphics and Visualization, Los Angeles, CA, 2004.

[13] Siira, J.; Pai, D. K.: Haptic texturing-A stochastic approach, Proceedings of the IEEE International Conference on Robotics and Automation, Los Alamitos, CA, 1996.

[14] Siira, J. O.; Pai, D. K.: Fast Haptic Textures, CHI Conference Companion, 1996.

[15] Costa, M.; Cutkosky, M.: Roughness Perception of Haptically Displayed Fractal Surfaces, Proc. ASME Dynamic Systems and Control Division, 2000.
[16] Vasudevan, H.; Manivannan, M.: Recordable Haptic Textures, HAVE2006, Ottawa, Canada, 4-5 November 2006, 130-133.
[17] Andrews, S.; Lang, J.: Interactive Scanning of Haptic Textures and Surface Compliance, Proceedings of The Sixth International Conference on 3-D Digital Imaging and Modeling, IEEE Computer Society, Washington, DC, USA, 2007, 99-106.
[18] Weiner, I. B., Ed.: Handbook of psychology, Experimental psychology New York: Wiley, 2002.
[19] Watt, A.; Watt, M.: Advanced animation and rendering techniques, theory and practice, New York, Addison Wesley, 1992.
[20] Klatzky, R. L.; Lederman S. J.; et al.: Feeling textures through a probe: Effects of probe and surface geometry and exploratory factors, Perception and Psychophysics, 65, 2003, 613-63.
[21] Thomas, T. R.: Rough surfaces, London Imperial College Press, 1999.